25. G. G. Wong *et al.*, *Science* **228**, 810 (1985).
26. V. Kruys *et al.*, unpublished data.
27. We are grateful to E. Declercq and A. Billiau for providing us the goat anti-human IBN-β antiserum and to the Glaxo Institute (Geneva) for sending us anti-human GM-CSF antiserum. This work was supported by ULB–Actions de Recherches Concertées of the Belgian Government and Crédit aux Chercheurs from the Belgian National Fund for Scientific Research to G.H. O.M. is supported by a grant from the Institute for Encouragement of Scientific Research in Industry and Agriculture.

17 February 1989; accepted 23 May 1989

Osteoclastic Bone Resorption by a Polarized Vacuolar Proton Pump

HARRY C. BLAIR, STEVEN L. TEITELBAUM, ROBERT GHISELLI, STEPHEN GLUCK*

Bone resorption depends on the formation, by osteoclasts, of an acidic extracellular compartment wherein matrix is degraded. The mechanism by which osteoclasts transport protons into that resorptive microenvironment was identified by means of adenosine triphosphate–dependent weak base accumulation in isolated osteoclast membrane vesicles, which exhibited substrate and inhibition properties characteristic of the vacuolar, electrogenic H^+-transporting adenosine triphosphatase (H^+-ATPase). Identity of the proton pump was confirmed by immunoblot of osteoclast membrane proteins probed with antibody to vacuolar H^+-ATPase isolated from bovine kidney. The osteoclast's H^+-ATPase was immunocytochemically localized to the cell-bone attachment site. Immunoelectron microscopy showed that the H^+-ATPase was present in the ruffled membrane, the resorptive organ of the cell.

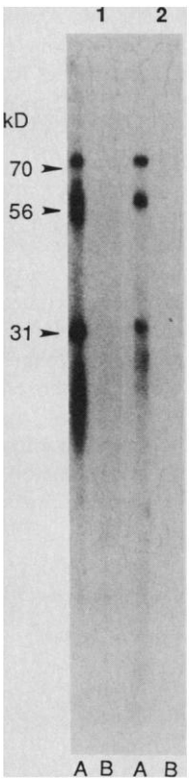

Fig. 2. Immunoblot of osteoclast microsomal proteins or purified bovine kidney H^+-ATPase probed with (lanes A) antiserum to H^+-ATPase or (lanes B) preimmune serum. Immunoreactivity of 70-, 56-, and 31-kD subunits seen in the kidney H^+-ATPase are also present in the osteoclast membranes. (Sample 1) Affinity-purified bovine kidney H^+-ATPase (5 μg) (*9*) and (sample 2) osteoclast microsomes (50 μg) were separated by SDS–polyacrylamide gel electrophoresis, transferred to nitrocellulose paper, and probed with antiserum or control serum as described (*9*); ^{125}I-labeled protein A and autoradiography were used for detection.

THE OSTEOCLAST, WHICH IS THE principal resorptive cell of the skeleton, degrades both the inorganic and organic components of bone in a localized area at its matrix attachment site. Although the complete mechanism by which the cell resorbs bone is unknown, it is believed to involve acidification of the osteoclast-bone interface (*1–3*). This hypothesis rests on the fact that bone mineral is hydroxyapatite, $Ca_3(PO_4)_2Ca(OH)_2$, an alkaline salt, and hence its dissolution requires protonation, ~2 moles of H^+ for each mole of Ca^{2+} placed into solution.

Baron *et al.* (*4*) reported that the cell's characteristic resorptive organ, the ruffled membrane, expresses on its extracellular domain a 100-kD protein that reacts with antibody to the vanadate-sensitive hydrogen and potassium-dependent adenosine triphosphatase (H^+,K^+-ATPase) of gastric parietal cells. We undertook experiments aimed at assessing the function of the osteoclast's H^+ transport system by exploiting the property of weak bases of low molecular mass to diffuse into acidic compartments where they are trapped by protonation, raising the *p*H (*5*). Starting with highly enriched (95% to 98% pure) populations of osteoclasts isolated from calcium-deprived laying hens (*6*), we produced membrane vesicles by differential centrifugation after homogenization of osteoclasts in isotonic sucrose buffer (7) and used acridine orange, a fluorescent weak base *p*H indicator, to determine proton transport in response to exogenous nucleoside triphosphate addition in the presence and absence of specific inhibitors (*7, 8*). We found that osteoclast membranes were capable of adenosine triphosphate (ATP)–dependent H^+ transport (Fig. 1). Vesicle acidification was not inhibited by 1 m*M* sodium orthovanadate, an agent that completely damps the gastric H^+,K^+- and other E_1E_2-type ATPases (*9*). The osteoclast's proton pump was also resistant to the mitochondrial H^+-ATPase inhibitor oligo-

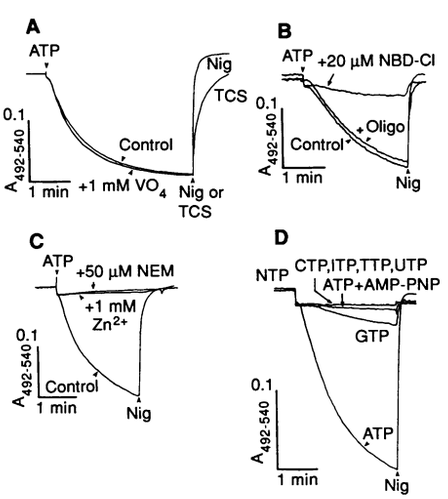

Fig. 1. ATP-dependent proton transport by isolated inside-out osteoclast membrane vesicles. Proton transport was assayed with a dual-wavelength spectrophotometer by monitoring uptake of acridine orange, as described (*6*), with 25 μg of membrane vesicles in 1 ml of buffer containing 150 m*M* KCl, 10 m*M* bis-tris-propane, 2 m*M* $MgCl_2$, and 1 μ*M* valinomycin, *p*H 7.0, and was initiated by the addition of 1 m*M* ATP (or other nucleotides, as described). The protonophores nigericin (Nig), 1 μm, or tetraclorosalicylanilide (TCS), 1 μm, were added as indicated. (**A**) Control, and with addition of 1 m*M* sodium orthovanadate; (**B**) control, with addition of oligomycin (5 μg/ml), and with addition of 20 μ*M* 7-chloro-4-nitrobenz-2-oxa-1,3-diazole (NBD-Cl); (**C**) control, with addition of 50 μ*M* *N*-ethylamleimide (NEM), and with addition of 1 m*M* $ZnCl_2$; and (**D**) 1 m*M* of each nucleotide [1 m*M* 5′-adenylylimide-diphosphate (AMP-PNP) was added prior to ATP addition]. Vesicles were prepared from 2×10^7 osteoclasts, obtained as described (*6*), homogenized in a Dounce homogenizer (20 strokes) in 15 ml of 250 m*M* sucrose, 5 m*M* tris, 1 m*M* EGTA, 1 m*M* $KHCO_3$, and 1 m*M* dithiothreitol, *p*H 7.0, at 4°C. After an initial centrifugation (1000*g* for 5 min), the supernatant was centrifuged (6000*g* for 15 min) to remove mitochondria and lysosomes. The supernatant was centrifuged at 42,000*g* for 30 min, and the upper, white microsomal layer of the pellet was collected. $A_{492\text{-}540}$, differences in absorbance at 492 nm and 540 nm.

H. C. Blair and R. Ghiselli, Department of Pathology, Jewish Hospital at Washington University Medical Center, St. Louis, MO 63110.
S. L. Teitelbaum, Department of Pathology, Jewish Hospital at Washington University Medical Center, St. Louis, MO 63110, and Shriners' Hospital for Crippled Children, St. Louis, MO 63130.
S. Gluck, Renal Division, Department of Medicine, Jewish Hospital at Washington University Medical Center, St. Louis, MO 63110.

*To whom correspondence and requests for reprints should be addressed.

mycin, but sensitive to *N*-ethylmaleimide and to 7-chloro-4-nitrobenz-2-oxa-1,3-diazole, properties characteristic of the vacuolar H^+-ATPases, including the bovine kidney vacuolar H^+-ATPase responsible for urinary acidification (*7*).

We isolated the bovine kidney proton pump and produced antiserum that reacts with its major cytoplasmic domain subunits, the 70-, 56-, and 31-kD polypeptides (*10*). We then prepared immunoblots of SDS-solubilized, electrophoretically separated osteoclast membranes with this antiserum and found immunoreactive polypeptides at 70, 56, and 31 kD, masses identical to those of the three major immunoreactive subunits of the kidney proton pump (Fig. 2). Thus by immunologic, structural, and functional criteria, proton-transporting osteoclast membranes have a vacuolar H^+-ATPase.

Vacuolar-type H^+-ATPase are found in endosomes, lysosomes, and several other intracellular compartments (*11*), as well as in the plasma membrane of some cells (*12*). The lysosomal proton pump was found earlier to use guanosine triphosphate (GTP) as a substrate nearly as effectively as ATP, whereas the endosomal H^+-ATPase appears to use only ATP (*13*). We found that ATP-stimulated proton transport into osteoclast membrane vesicles was approximately ten times as fast as GTP-stimulated acidification (Fig. 1). We could not therefore exclude the possibility that the proton pump–bearing osteoclast membranes were derived from a compartment within the resorptive cell rather than from the ruffled border.

We therefore investigated the cellular distribution of the osteoclastic H^+-ATPase by probing histological sections of chicken medullary bone with affinity-purified antibodies to the major subunits of the bovine kidney H^+-ATPase. Intense staining of osteoclasts was observed, and in most cells the antibody was localized at the bone attachment site (Fig. 3, A and B). Some osteoclasts (~5%) contained immunoreactive material throughout their cytoplasm. These cells were all either unattached to bone or juxtaposed to osteoid (nonmineralized matrix), suggesting that bone mineral may prompt polarized expression of proton pump at the resorptive microenvironment. Such redistribution of proton pump be-

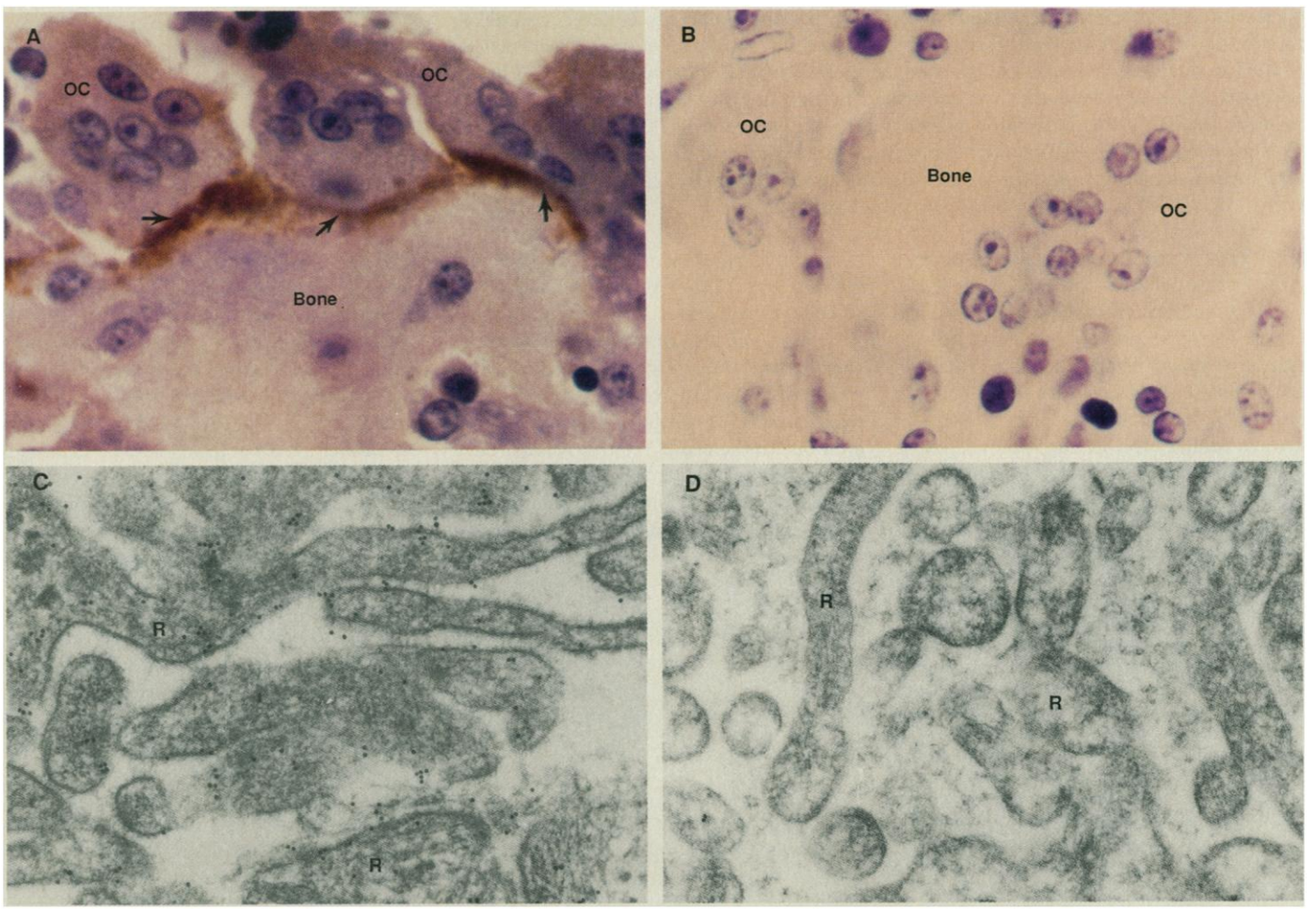

Fig. 3. Vacuolar H^+ pump visualized by in situ immunocytochemistry at the resorptive surface of osteoclasts. (**A**) Indirect peroxidase staining of affinity-purified rabbit antibody to the 31-kD subunit of bovine vacuolar ATPase (*9*), showing its localization of the cell-bone attachment site, and (**C**) protein A–gold binding at the ruffled membrane of osteoclasts reacted with affinity-purified antibody to whole bovine vacuolar ATPase, representing an area similar to that at the arrow in (A) but magnified ~40 times more (*9*). (**B**) and (**D**) represent appropriate controls with preimmune sera. Medullary bone from calcium-deprived laying hens (*6*) was fixed in 4% Formalin with 0.2*M* $HgCl_2$ and 0.15*M* sodium acetate (A and B) or 4% formaldehyde, 0.1% glutaraldehyde, 0.1*M* cacodylate, *p*H 7.4 (C and D) (*3*), followed by paraffin embedding, sectioning, and antibody incubation. Bound antibody was visualized with biotinylated goat antibody to rabbit serum and was peroxidase-labeled with an avidin-biotin complex (A and B). Alternatively, 500-μm sections of ammonium chloride–washed wet tissue was incubated overnight in phosphate-buffered saline with rabbit antibodies; washing, dehydration, plastic embedding, sectioning for electron microscopy was done as before, and bound antibody was visualized by reaction of thin sections with 10 nm of protein A–gold (C and D). Sections were counterstained with hematoxylin (A and B) or osmium tetroxide, uranyl acetate, and lead citrate (C and D). Arrows indicate antibody binding at the osteoclast-bone attachment site. OC, osteoclasts; R, ruffled membrane. Nuclei in (A) and (B) are ~3 μm. Gold in (C) and (D)is 10 nm in diameter.

tween cytoplasm and cell membrane has been demonstrated in proton-secreting renal epithelial cells (*14*). In keeping with evidence that resorptive cells do not effectively attach to unmineralized bone matrix (*15*), H^+-ATPase was absent at all sites where osteoclasts were juxtaposed to osteoid (unmineralized bone). Finally, we used immunoelectron microscopy to show that the ruffled border, the highly convoluted cell membrane characterizing the site of bone resorption, contains the H^+-ATPase (Fig. 3, C and D).

Thus, the osteoclast has a vacuolar-type proton pump that is physiologically and structurally identical to the kidney H^+-ATPase and that appears to be responsible for creation of the acidic microenvironment fundamental to bone resorption. The osteoclast's ruffled membrane has a dense array of cytoplasmic proteinaceous studs (*16*) similar to those found on the plasma membrane of renal proton-transporting epithelia, which represent the cytoplasmic domain of the vacuolar H^+-ATPase (*17*). As in the kidney intercalated cell, osteoclastic proton pumps are polarized to one plasma membrane domain, allowing vectorial proton secretion. The mechanism by which the osteoclast maintains the polarity of the proton pump at the osteoclast-bone interface is unknown and is an intriguing problem, since osteoclasts, unlike epithelial cells, do not form tight junctions. However, when epithelial cells attach to substrate, polarization begins before the formation of tight junctions and is associated with cytoskeletal reorganization (*18*). The development of the osteoclastic attachment site, which is rich in cytoskeletal elements, may represent a similar polarization process.

REFERENCES AND NOTES

1. A. Cretin, *Presse Med.* **59**, 1240 (1951).
2. M. D. Fallon, *Endocrine Control of Bone and Calcium Metabolism*, C. V. Conn, T. Fujita, J. R. Potts, Jr., R. V. Talmage, Eds. (Elsevier, Amsterdam, 1984), vol. 8A, pp. 144–146.
3. R. Baron, L. Neff, P. J. Courtnoy, *J. Cell Biol.* **101**, 2210 (1985).
4. R. Baron, L. Neff, C. Roy, A. Bolsvert, M. Caplan, *Cell* **46**, 311 (1986).
5. C. DeDuve *et al.*, *Biochem. Pharmacol.* **23**, 2495 (1974).
6. H. C. Blair, A. J. Kahn, E. C. Crouch, J. J. Jeffrey, S. L. Teitelbaum, *J. Cell Biol.* **102** 1164 (1986).
7. S. Gluck and Q. Al-Awqati, *J. Clin. Invest.* **73**, 1704 (1984).
8. J. Glickman, K. Croen, S. Kelly, Q. Al-Awqati, *J. Cell Biol.* **97**, 1303 (1983).
9. L. Faller *et al.*, *Ann. N.Y. Acad. Sci.* **402**, 146 (1982).
10. S. Gluck and J. Caldwell, *J. Biol. Chem.* **262**, 15780 (1982).
11. S. Ohkuma, Y. Moriyama, T. Tatsuy, *Proc. Natl. Acad. Sci. U.S.A.* **79**, 2758 (1982).
12. I. Mellman, R. Fuchs, A. Helenius, *Annu. Rev. Biochem.* **55**, 663 (1986).
13. C. J. Galloway, G. E. Dean, G. Rudnick, I. Mellman, *Proc. Natl. Acad. Sci. U.S.A.* **80**, 3334 (1983).
14. S. Gluck *et al.*, *ibid.* **79**, 4327 (1982).
15. J. Jonesey, *J. Clin. Invest.* **51**, 9 (1972); Z. Bar-Shavit *et al.*, *ibid.* **72**, 526 (1983).
16. S. L. Teitelbaum, C. C. Stewart, A. J. Kahn, *Calcif. Tissue Int.* **27**, 255 (1979).
17. D. Brown, S. Gluck, J. Hartwig, *J. Cell Biol.* **105**, 1637 (1987).
18. K. Simons and S. Fuller, *Annu. Rev. Cell Biol.* **1**, 243 (1985).

19. We thank J. Konsek and R. Henry for technical assistance. Supported by NIH grants AM01631 (to H.C.B.), AM32788 (to S.L.T.), and AM34788 (to S.G.) and a grant from the Shriners' Hospital for Crippled Children, St. Louis Unit. This work was done during the tenure of an established investigatorship award from the American Heart Association and Sandoz Pharmaceuticals Corporation (to S.G.).

28 April 1989; accepted 23 May 1989

Role of Prostaglandins and cAMP in the Secretory Effects of Cholera Toxin

JOHNNY W. PETERSON AND LAURA G. OCHOA

The role of adenosine 3′,5′-monophosphate (cAMP) and prostaglandins in the pathogenesis of experimental cholera was evaluated. Fluid accumulated in the rabbit intestinal loop model after 16 hours of incubation with cholera toxin, prostaglandin E_1, or prostaglandin E_2, but not with membrane-permeable derivatives of cAMP or forskolin. Dibutyryl cAMP triggered a small, transient intestinal fluid accumulation response by 4.5 hours; however, the fluid was completely absorbed by 9 hours. After exposure of intestinal loops to cholera toxin, prostaglandin E was released into the intestinal lumen in a concentration-dependent manner independent of cAMP. Thus, not only cAMP, but also prostaglandins may regulate water and electrolyte secretion in cholera.

THE PATHOGENIC MECHANISM OF cholera and several other intestinal enteropathies caused by *Escherichia coli*, *Salmonella* species, *Campylobacter jejuni*, and other enterotoxin-producing bacteria is thought to be mediated by cAMP (*1*). The A_1 subunit of cholera toxin possesses both nicotinamide adenine dinucleotide glycohydrolase and adenosine diphosphate (ADP)–ribosyltransferase activities. Cholera toxin catalyzes the ADP-ribosylation of the α subunit of the stimulatory G protein ($G_{s\alpha}$) of adenylate cyclase (*2*). The guanosine triphosphate–binding activity of $G_{s\alpha}$ is altered by covalent linkage to ADP-ribose, which causes the catalytic site of adenylate cyclase to increase cAMP production. The cAMP content of cholera toxin–affected cells increases markedly and in proportion to the amount of cholera toxin stimulation (*3*).

Clinically, the only important cell types naturally affected by cholera toxin reside in the intestinal mucosa. After exposure to cholera toxin, the cAMP content of the crypt epithelial cells of the small intestine increases, and water and electrolyte transport is altered (*4, 5*). Application of dibutyryl cAMP to stripped intestinal mucosa in Ussing chambers increases chloride ion transport (*4*). Thus, fluid and electrolyte loss in cholera patients is associated with increased cAMP concentrations.

We have reevaluated the cause-effect relation of cAMP formation, prostaglandin E (PGE) release, and intestinal fluid secretion. The possible participation of prostaglandins in the pathogenesis of cholera was suggested by Bennett (*6*); both PGE_1 and PGE_2 stimulate intestinal adenylate cyclase (*7*). The effects of cholera toxin on secretion and on cAMP accumulation are inhibited by drugs that inhibit prostaglandin formation (for example, indomethacin, aspirin, and ibuprofen) (*8–11*). The PGE_2 content of jejunal aspirates from individuals with acute cholera is significantly higher than in those from convalescent patients (*12*). Concentrations of PGE increase in the intestinal mucosa of rabbits challenged with cholera toxin, *Vibrio cholerae*, or *Salmonella* species (*13*). Cholera toxin also increases the release of PGE_2 and 5-hydroxytryptamine in rat jejunal segments (*14, 15*). A murine macrophage cell line releases PGE_2 when exposed to either cholera toxin or pertussis toxin, but not when exposed to dibutyryl cAMP (*16*). We used the rabbit intestinal loop model (*17*) to investigate the relation of cAMP and PGE to the cholera toxin–mediated secretory response.

To compare the effects of cAMP, PGE, and cholera toxin on net fluid secretion, we injected the lumina of rabbit intestinal segments with various agents (*18*) and measured the mean fluid accumulation responses of intestinal loops after an overnight (16 hours) exposure (Table 1). Cholera toxin caused approximately 1.5 ml of fluid per centimeter of intestine to accumulate. When

Department of Microbiology, University of Texas Medical Branch, Galveston, TX 77550.